CrystEngComm

Accepted Manuscript

ROYAL SOCIETY OF CHEMISTRY

www.rsc.org/crystengcomm

Journal Name

RSCPublishing

ARTICLE

Tröger's Base Quasiracemates and Crystal Packing Tendencies‡

Cite this: DOI: 10.1039/x0xx00000x

Jacob T. Cross,[a] Nicholas A. Rossi,[a] Mateusz Serafin[a] and Kraig A. Wheeler[a]*

Received 00th January 2012,
Accepted 00th January 2012

DOI: 10.1039/x0xx00000x

www.rsc.org

A family of 7 Tröger's base (TB) compounds that vary in configuration (quasiracemates, racemates, and enantiomers) and chemical substitutions (Me, Cl, and Br) has been investigated. The deliberate use of isosteric components provided a logical entry point to explore the quasiracemic behavior of TB compounds. Crystal structures of these quasiracemates contain several sets of molecular dimers organized by the complementary topologies of the quasienantiomeric components. These motifs closely mimic the local inversion symmetry environment observed with the racemic and solid-solution phases included with this study. Comparing this set of crystal structures to 105 TB entries found in the Cambridge Structural Database revealed four distinct dimeric packing patterns retrieved using TB···TB distance and orientation search criteria. Each motif takes advantage of the complementary topologies of the V-shaped building blocks and further highlights the importance of molecular shape to the recognition profile of these supramolecular assemblies. This approach exposed 58% of the entries (65 structures) exhibiting one or more of the pairwise relationships. Furthermore, sorting the entries based on centrosymmetric and noncentrosymmetric space groups provided evidence for a correlation between motif and crystallographic symmetry.

Introduction

This year marks the 100th anniversary of the discovery of X-ray crystallography. Many recent reports reflect on the impact of this discipline to the scientific community and offer important discussions that highlight new technology and uses of crystallographic data.[1] The rich history of crystallography is steeped in the early days of the father and son team W. H. and W. L. Bragg, where they recognised periodic materials could offer critical insight to the utility of X-ray diffraction.[2] As is now well understood, such studies ultimately proved quite valuable for determining the underlying structure for a wide variety of crystalline materials. These early contributions have not gone unnoticed, but rather anchor a vibrant community of practitioners that continue to pursue weighty critical scientific outcomes. Over the last hundred years, the technique of interpreting diffraction patterns produced from the interplay of focused radiation sources and crystal periodicity has delivered ground-breaking changes to the way we reason and practice science. The collection of prominent highlights from crystallographic investigations is extensive with many seminal innovations to report. Though some of the most recognizable discoveries involve singular crystal structures such as DNA,[3] hemoglobin,[4] penicillin,[5] and Vitamin B12[6] to name a few, the use and impact of crystallographic data to uncover the fundemental properties of materials has been undeniably central to many scientific disciplines. For example, the early concepts of atomic periodicity[7] (*e.g.* bond order and atomic radii), aromaticity,[8] and absolute configuration[9] were each developed with the support of X-ray diffraction experiments leading to important paradigm shifts in chemical thinking. While moving from single reports to finding meaning in collections of related crystals structures provides a well-trodden path for today's researchers, this discipline was largely undiscovered until the early 1970's with the development of the field of structural systematics.[10]

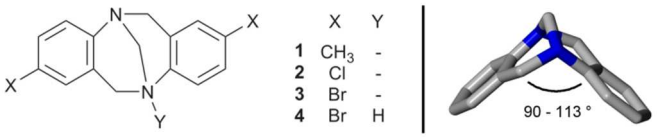

Scheme 1. Tröger's base adducts for this study (left) and a 3D view of the framework showing the range of cleft angles retrieved from the extant crystallography database (right).

Tröger's base (TB), (*rac*)-**1**, has also experienced a distinguished past dating back to 1887 with the publication of Julius Tröger's doctoral dissertation from the University of Leipzig.[11] Several recent reviews[12] detail the historical journey

of this compound starting with Tröger's own assignment of (±)-**1** as a 'base $C_{17}H_{18}N_2^+$'. While considerable effort was directed at identifying a suitable chemical framework for Tröger's compound it was not until 1935, some fifty years after its discovery, that Spielman using chemical reactivity patterns correctly proposed the structure as 2,8-dimethyl-6*H*,12*H*-5,11-methanodibenzo[*b*,*f*][1,5]diazocine (**1**).[13] Given the ease of crystallization of **1** and steady interest with X-ray diffraction it is somewhat surprising that an additional fifty years passed before the structure of TB was confirmed by crystallographic methods.[14] Since then the chemistry and application of TB compounds have been actively pursued giving way to a sizable collection of literature reports.

The recent interest with **1** and its derivatives is firmly linked to the core 1,5-diazabicyclo[1.3.3]nonane framework. This molecular architecture and the two aryl attachments produce a rigid V-shaped molecule with a cleft angle of 99(5)° (Scheme 1, right).[15] Such a molecular topology combined with inherent C2-symmetric chirality, framework stability, and relative ease of preparation and derivatization offers an attractive starting point for a variety of functional materials. For example, the areas of molecular recognition,[16] chiral separations,[17] asymmetric catalysts,[18] and functional nanoporous materials[19] have all benefited from principal components derived from TB compounds.

As evident from growing interest with the chemistry of TB compounds, the field has now progressed to an established science, supported by an extensive library of robust synthetic protocols. These synthetic developments promote the availability of a diverse group of molecular scaffolds (*e.g.*, symmetric, asymmetric, fused, and highly functionalised) that has in turn permitted the field to adapt to a wide range of functional materials. Though the recognition of TB compounds and various guest molecules continues to hold considerable interest, it is notable to mention that the packing preferences of TB have yet to be thoroughly explored. This contribution celebrates the centennial anniversary of X-ray crystallography by examining the crystal structures and recognition profiles of a homologous family of 2,8-disubstituted TB compounds (**1** - **4**) (ESI†). The initial motivation for this study focused on applying the quasiracemic approach to TB frameworks. Crystal structures gleaned using this strategy were also combined with several new racemic and enantiomeric phases and 105 TB structures retrieved from the current crystallographic database. Exploring common structural motifs that emerge from these investigations offers critical insight to understanding the rich structural chemistry of this class of compound. Moreover, emphasizing how the V-shaped topology of TB transfers to crystal alignment, outcomes from this study should be of interest to the design of functional TB imprinted materials.

Molecular Recognition of Tröger Base Adducts

Tröger base molecules continue to provide fertile ground for a wide range of supramolecular disciplines. One emergent theme from these studies includes decorating the aryl group of the tweezer framework with a variety of functional groups. This effort has allowed the development of receptor systems capable of recognizing tailor-made guest molecules. While many of these newly reported multimolecular assemblies have been isolated and crystallographically characterized, the aim of these studies is often firmly grounded in exploring the observed inclusion behaviour or targeted chemical process. As expected, this collective effort offered only cursory attention to decoding the preferred recognition profiles that exist between TB units. When considering the core framework of the TB building block, the lack of conventional hydrogen-bond donor groups likely translates to crystal organization due to a blend of weak electrostatic interactions and best-fit scenarios. Building on the curious molecular shape features of TB, the selection of compounds **1** – **3** for this study provides accessible targets that, when recrystallized, assemble without the help of strong intermolecular interactions.

Over the last several years our group has pursued quasiracemic materials as a structural tool for probing the role of molecular shape to the organization of supramolecular arrays.[20] These materials consist of equimolar portions of isosteric chemically unique compounds of opposite handedness. Brock *et al.* recently reported a survey of 114 quasiracemic compounds from the literature.[21] All but one (MIYGAC[22], a diastereomeric pair of quasienantiomers) organize in molecular crystals with approximate inversion relationships that mimic the structures of the corresponding racemates. This structural preference follows Kitaigorodskii's close packing principle.[23] In the case of quasiracemates, the notion of close packing is related to the affinity of the quasienantiomers. When assembled pairwise, the complementarity of the left and right-handed components best achieve enthalpically preferred motifs using near centrosymmetric related packing. The supramolecular control and asymmetry that accompanies quasiracemic materials continues to provide an important platform for the identification,[24] asymmetric catalysis,[25] kinetic resolution,[26] enantiomeric enrichment[27] and polar alignment[28] of small molecule species.

In the context of this study the quasiracemic design strategy was applied to the TB framework to understand the preferred recognition profiles of these systems. Adducts containing 2,8-disubstituted frameworks (Scheme 1; X = Me, Cl, and Br) were used to construct quasiracemates (*R,R*)-**1**/(*S,S*)-**2** and (*S,S*)-**2**/(*R,R*)-**3**. During the course of investigation we also uncovered several new racemic [(*rac*)-**2**-I, (*rac*)-**2**-II,], enantiomeric [(*S,S*)-**4**], and solid solution [(*S,S*)-**1**/(*S,S*)-**2**, (*S,S*)-**1**/(*rac*)-**3**] phases that contribute directly to the structural underpinnings of this discussion. Inspection of this collection of structures combined with the extant Cambridge Structural Database[29] (CSD, Version 5.35, November 2013) entries revealed four prominent packing motifs, *i.e.,* M1 – M4 (Scheme 2). Though both motifs M1 and M2 have been previously reported for related molecular cleft compounds, to our knowledge a systematic search identifying preferred TB···TB interactions has yet to be investigated.[30]

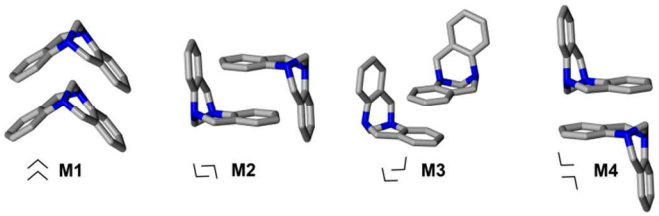

Scheme 2. Preferred alignment of Tröger's base dimeric assemblies.

Molecular associations described as M1 – M4 arise from a complex blend of TB contacts and structural features. Though molecular topology certainly plays a prominent role in motif construction, weak cohesive intermolecular forces such as aryl edge-to-face (C-H···π) and aryl offset face-to-face (π···π) also contribute.[31] In the case of M1, such assemblies are constructed from columns of two or more components with the apex of one molecule suitably aligned in the cleft of a second. Motifs M2 and M3 arise from the insertion of an aryl group of one molecule into the cleft of another *via endo*-face to *endo*-face or *end*-face to *exo*-face interactions, respectively. The last pattern, M4, aligns the topside aryl surfaces of the TB components. Closely aligned M4 motifs occur by use of pairs of *exo*-face to *exo*-face coplanar assembles. When considering the effect of molecular topology to supramolecular assembly, each of these motifs offers important opportunities for close packing of the building blocks.

The crystal structures of the quasiracemic systems are shown in Figs. 1 and 2. For (*R,R*)-**1**/(*S,S*)-**2**, the quasienantiomeric components differ by Me and Cl substitutions and organize with a molecule of solvent, acetone, in the asymmetric unit (space group $P2_12_12$). In this structure the affinity for quasienantiomeric molecular shapes is best accommodated by use of M2 and M4 motifs. The near centrosymmetric M4 assemblies consist of pairs of (*R,R*)-**1** and (*S,S*)-**2** components, while the M2 motif is made up of combinations of two-fold rotation related (*R,R*)-**1** or (*S,S*)-**2** molecules skewed by ~20°. Quasiracemate (*R,R*)-**2**/(*S,S*)-**3** incorporates the Cl and Br groups and, despite identical recrystallization conditions to quasiracemate **1**/**2**, leads to an anhydrate phase in space group *P*1 (Fig. 2). Comparing the crystal packing and unit cell parameters of (*S,S*)-**2**/(*R,R*)-**3** to the 2,8-dibromo (XENGIH)[32] and 2-bromo-8-methyl (NUHGED)[33] racemic phases indicates a high degree of isostructurality. Fig. 2 shows the two chemically unique components organized by a mixture of Type II[34] Cl···Cl (3.68Å) and Br···Br (3.62Å) contacts resulting in homomeric molecular chains that propagate along the *c* axis. Neighboring chains further organize in this system to give approximate inversion related M2 and M4 motifs constructed from pairs of (*S,S*)-**2** and (*R,R*)-**3** molecules.

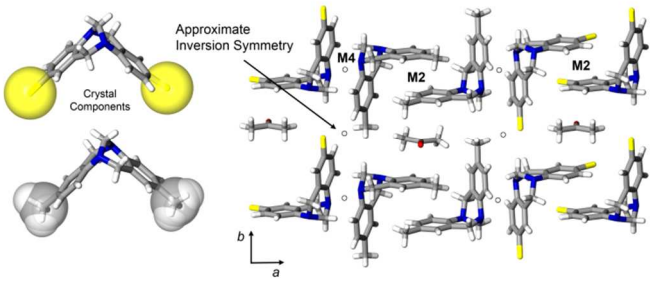

Fig. 1 Crystal structure of quasiracemate (*R,R*)-**1**/(*S,S*)-**2**·acetone showing isosteric Me and Cl components organized with near centrosymmetric alignment.

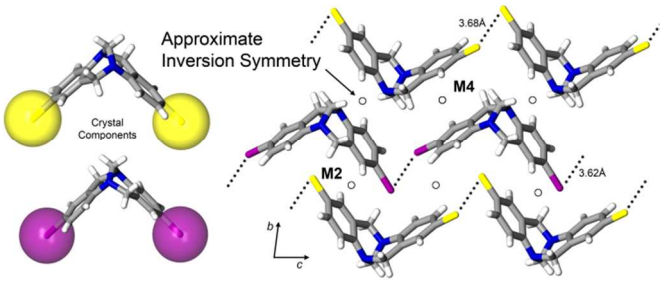

Fig. 2 Crystal structure of quasiracemate (*S,S*)-**2**/(*R,R*)-**3** showing isosteric Cl and Br components organized with near centrosymmetric alignment and Cl···Cl and Br···Br interactions.

As an avenue to further probe the structural preferences of TB molecules, we prepared the bimolecular compounds (*S,S*)-**1**/(*S,S*)-**2** and (*S,S*)-**1**/(*rac*)-**3**. Given the isosteric nature of the Me, Cl, and Br functional groups, it is not surprising that when combined with the imposed molecular configurations, the result is solid-solution crystalline phases where the components coexist in an unordered manner in the crystal lattice. Both systems, (*S,S*)-**1**/(*S,S*)-**2** and (*S,S*)-**1**/(*rac*)-**3**, were prepared by co-crystallization of equimolar portions of the building blocks; even so, crystals selected for the study lack an even distribution of components. This was determined by refinement of the occupancy factors associated with the disordered fragments to give a 32:68 ratio for Me:Cl [(*S,S*)-**1**/(*S,S*)-**2**] and a 60:40 ratio for Me:Br [(*S,S*)-**1**/(*rac*)-**3**]. Crystals of (*S,S*)-**1**/(*S,S*)-**2** form in space group $P2_12_12_1$ and despite disorder of the CH_3/Cl site exhibit an infinite set of perpendicular Cl···Cl interactions (3.47Å, Type II) along the *a* axis (Fig. 3). The crystal packing of the (*S,S*)-**1** and (*S,S*)-**2** components lacks any detectable M1 – M4 motifs. Crystals of (*S,S*)-**1**/(*rac*)-**3** form in space group *P*1 and display near inversion M2 and M4 relationships (Fig. 4). This phase is isostructural with quasiracemate (*S,S*)-**2**/(*R,R*)-**3** and the CSD entries XENGIH and NUHGED. While the (*R,R*)-**3** component is well ordered, the enantiomeric counterpart consists of disorded CH_3 and Br substituents. Interestingly, both the (*R,R*)-**3** ordered sites participate in close Type II Br···Br contacts (3.68Å) as well as the partially occupied (*S,S*)-**3** bromine site (3.66Å).

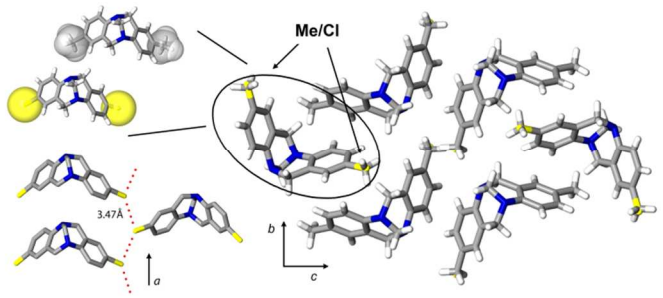

Fig. 3 Crystal structure of (*S,S*)-**1**/(*S,S*)-**2** indicating disordered components and Cl···Cl contacts.

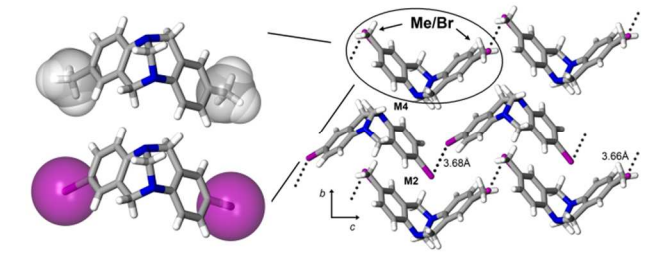

Fig. 4 Crystal structure of (*S,S*)-**1**/(*rac*)-**3** indicating the disordered (*S,S*) components and Br···Br contacts.

The crystal structure of (*rac*)-**2** has been previously reported with molecular dimers related by centrosymmetrically related M2 and M4 motifs.[35] Additional crystal growth experiments in our laboratory *via* slow evaporation of acetone and methanol solutions resulted in two new polymorphic phases - (*rac*)-**2**-I and (*rac*)-**2**-II, respectively. Inspection of Fig. 5 reveals the structure of (*rac*)-**2**-I with two symmetry independent molecules (Z' = 2) organized in space group $P\bar{1}$ forming columns of *endo*-face to *exo*-face M3 interactions that assemble along the *a*-axis. These assemblies are constructed of alternating symmetry independent molecules of the same chirality and link to adjacent centrosymmetrically related motifs by a mixture of Type I (3.51Å) and Type II (3.45Å) Cl···Cl interactions. For (*rac*)-**2**-II, molecules organize in space group $P2_1/n$ with centrosymmetrically related M2 dimers (Fig. 6). Though Fig. 6 seems to indicate the presence of M4 interactions, close inspection of these contacts reveals pairs of aligned molecules skewed from planarity by 56.2°.

On one occasion crystals of (*S,S*)-**4**·Cl were isolated from an HCl acidified chloroform solution of (*S,S*)-**3**. Crystallographic assessment of this sample showed the inclusion of solvent ($CHCl_3$) with components assembled using discrete N^+-H···Cl^- (N···Cl, 2.955(5)Å; N-H···Cl, 167(7)°) interactions accompanied by additional Br···Br contacts (3.47Å, Type II) (Fig. 7). The construction of this structure lacks any noticeable M1–M4 motifs.

Beyond the near approximate inversion relationships observed for the quasiracemic and racemic phases, no clear reliable packing motif emerges from this set of 7 crystal structures. Four entries exhibit M2 or M4 motifs [(*R,R*)-**1**/(*S,S*)-**2**, (*S,S*)-**2**/(*R,R*)-**3**, (*S,S*)-**1**/(*rac*)-**3**, (*rac*)-**2**-II], while only one structure organizes molecules with M3 alignment [(*rac*)-**2**-I]. None of these structures show the M1 motif and 2 lack any convincing correlation to motifs M1 – M4 [(*S,S*)-**1**/(*S,S*)-**2**, (*S,S*)-**4**·Cl]. Though conceptually using secondary molecules (*e.g.* guest-host systems and solvates) could impede the assembly of TB compounds, the two solvated structures [(*R,R*)-**1**/(*S,S*)-**2**, (*S,S*)-**4**·Cl] suggests this is not a fast rule. Certainly the family of structures selected here lacks breadth; nonetheless, perhaps one structural theme that begins to surface is the use of halogen···halogen and π-stacking interactions for crystal cohesion. Given the rigid framework and substitution pattern of this family, use of these non-bonded contacts to direct supramolecular architectures is an expected outcome.

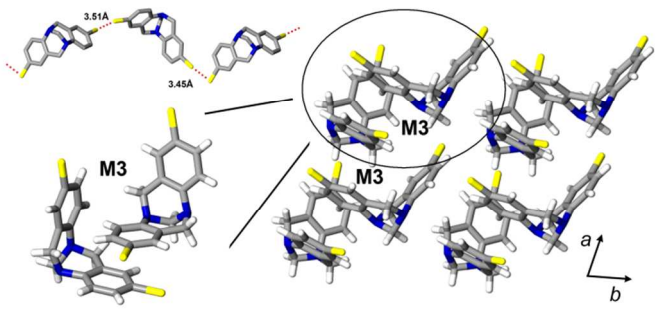

Fig. 5 Crystal structure of (*rac*)-**2**-I showing the assembly of M3 motifs and Cl···Cl contacts.

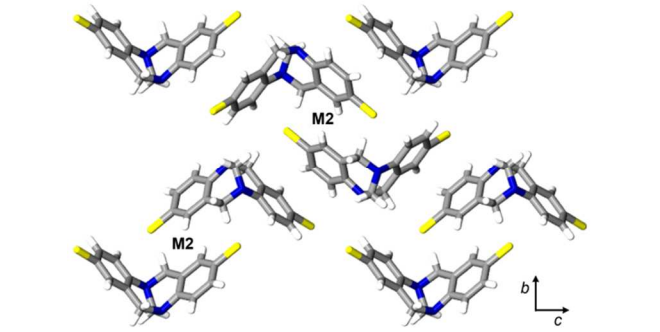

Fig. 6 Crystal structure of (*rac*)-**2**-II displaying M2 motifs.

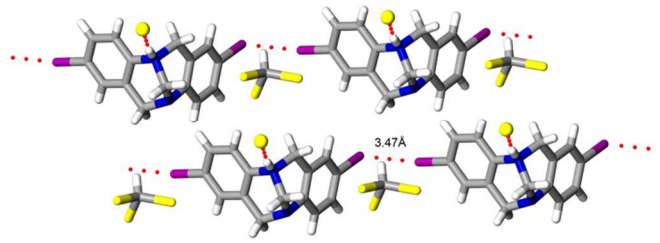

Fig. 7 Crystal packing diagram of (*S,S*)-**4**·Cl chloroform solvate showing molecular alignment and N^+-H···Cl^- and Br···Br contacts.

Mechanistic Details of Tröger's Base Formation

The mechanism of TB production has been the topic of extensive discussion since it was first synthesized over 125

years ago. From these early years with only limited tools for structure elucidation, Julius Tröger and many others encountered a formidable challenge assigning the correct structural identity of the TB core scaffold. Much of this challenge was likely related to the simplicity of starting materials – *i.e.,* aniline and a suitable methylene synthetic equivalent under acidic conditions – coupled with the formation of an unusual product framework. We now know the synthesis of **1** from these early efforts included the condensation of a 2:3 ratio of *p*-toluidine and methylal to give a bridged diazocine framework.

The mechanism depicted in Fig. 8 is generally accepted as the pathway to TB formation.[36] This process involves several key steps that include three successive methylene additions and two annulations. Wärnmark's recent description of this process cites the rate determining step as the conversion of tetrahydroquinone **6** into reactive intermediate **7**.[12a] Reducing the nucleophilicity of the aniline by use of an electron withdrawing group (*e.g.* halogen) can impede methylene addition and thus serve as a potential pathway to dihydroquinazoline **8**. In the course of studies towards the synthesis of (*rac*)-**2** we observed the formation of crystals corresponding to 6-chloro-3-(4-chlorophenyl)-3,3-dihydroquinazoline (**8**-Cl). The notion of capturing one of the intermediates on the path to TB is supported by the crystal structure of **8**-Cl as well as the previously reported structures of the dimethyl[37] and dimethyl ester[38] derivatives. This structural information, in connection with extensive mass spectrometry studies,[39] offers considerable opportunity to support (or contradict) current theories of chemical processes.

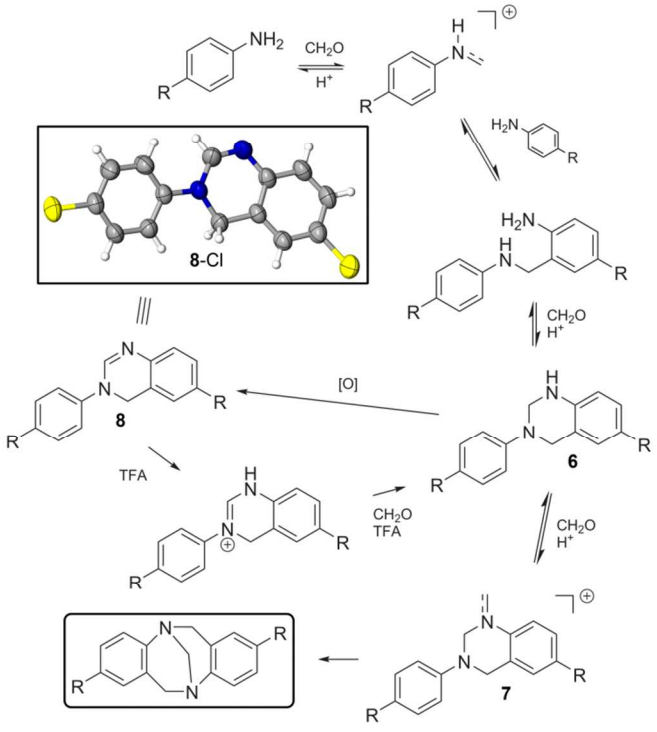

Fig. 8 Mechanistic process depicting the formation of Tröger's base adducts and crystal structure of intermediate **8**-Cl.

Crystal Structure Correlation

To understand the extent of transferability of packing motifs observed for **1** - **3**, we then turned our attention to the current database of TB crystal structures. A comparison of these structures offers an important opportunity to probe the packing preference of these rigid molecular tweezer compounds.

A search of the CSD consisted of the TB methanodibenzo diazocine core and excluded those entries with oligo TB compounds and substituents attached to the central bridging methylene group. No further attempt was made to filter structures based on the degree of derivatization or inclusion behavior (*e.g.,* guest-host systems and solvates). This data mining strategy retrieved 105 entries from the CSD, that when combined with the structures from the present work, offers a considerable database of 112 structures to explore the structural preferences of TB systems.

Given this collection of structures we wondered if it might be possible to devise a diagnostic tool to help recognise and assess TB···TB packing motifs. Inspection of Fig. 9A indicates the structural parameters used to differentiate motifs M1 - M4 (Scheme 2). Each parameter describes a relationship between pairs of neighboring TB molecules and includes:

D1	apex···centroid distance (defined by the midpoint of the 2 and 8 aryl carbon sites) (Å);
D2	apex···apex distance (Å);
D3	centroid···centroid distance (Å);
CC	aryl centroid···aryl centroid distance (Å); and
ϕ	relative orientation of neighboring molecules (°).

Differentiating the structural subtleties of motifs M1 – M4 seems feasible when considering the search criteria applied to this study. For example, pairs of molecules that display M1 alignment should give relatively short D1 distances, similar D2 and D3 values, and ϕ angles near 0°. By contrast, molecules exhibiting M2 and M4 alignment will approach ϕ = 180°, with positive D2-D3 values for M2 motifs and negative for M4. Tabulating these parameters and limiting the dataset of 112 structures to D1 < 8Å and D2 < 12Å gave a considerable database of 490 hits to explore. Taking advantage of the Data Analysis module contained in the CCDC Mercury software package[40] (version 3.3) allowed easy access to crystallographic data mining and 3D plots. Fig. 9B shows a plot of the 490 hits as D2-D3 vs. D1 with the relative orientation of molecules (ϕ) included as color shading. Though there appears some clustering of the data (*e.g.* D2-D3 ~ 0°), the lack of well-defined patterns can likely be ascribed to subtle variations in M1 – M4 motifs and also the continuum of molecular orientations that define the pairwise association of TB···TB motifs. Even so, the patterns of M1 – M4 begin to emerge when systematic filters are applied. Sorting the data for only entries with ϕ < 40° effectively exposes 182 molecular pair

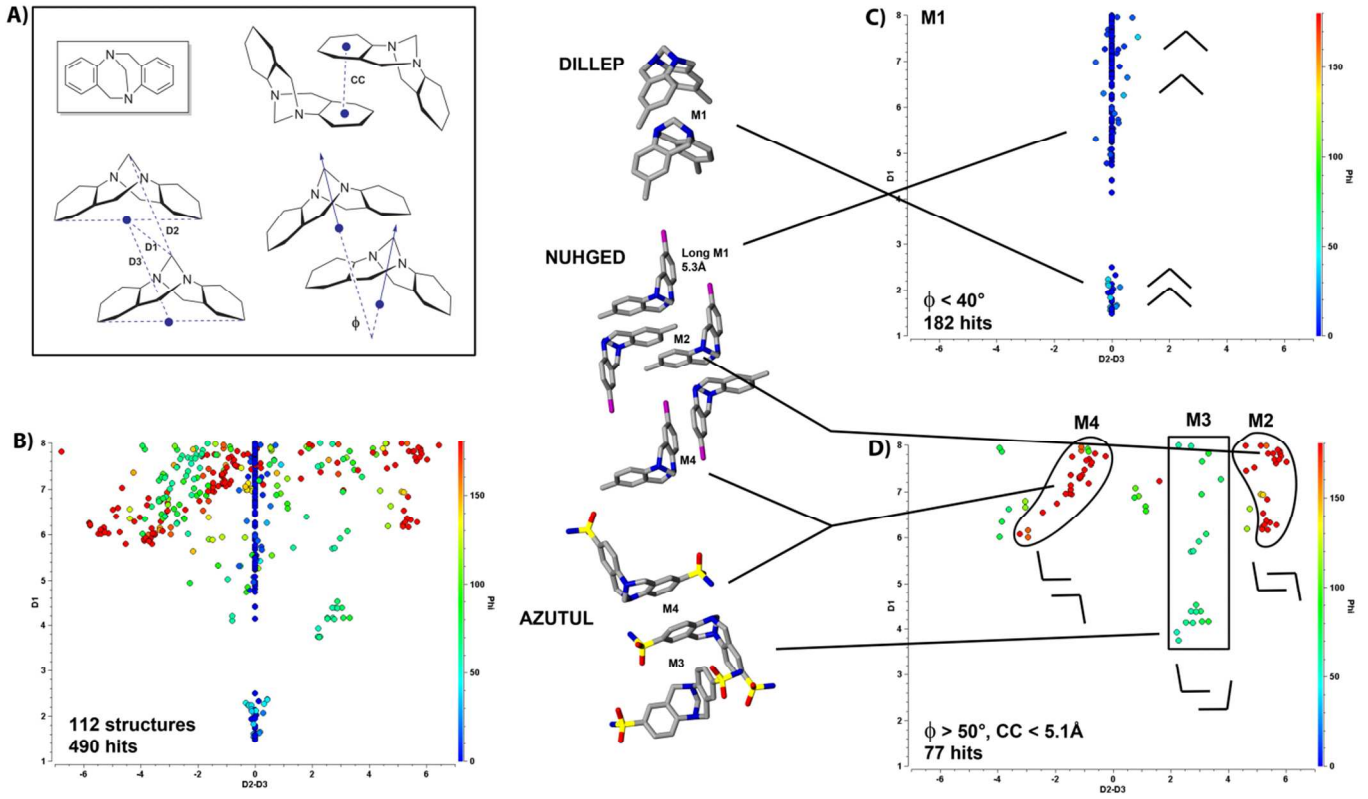

Fig. 9 Crystallographic database survey for Tröger's base supramolecular dimeric assemblies showing A) search criteria, B) complete data set, C) M1 motifs, and D) M2-M4 motifs.

associations that display M1 alignment (Fig. 9C). The distinct cluster at D1 < 3Å (33 hits, 27 refcodes) corresponds to the pairwise approach of TBU assemblies *via* the close interaction of apex···molecular cleft contacts. The original 1986 structure of Tröger's base - (*rac*)-**1**, DILLEP - exhibits two short M1 contacts with D1 = 1.53 and 1.63 Å (Fig. 9C).[14] Additionally, inspection of those entries D1 values above 4Å reveals structures with M1 interactions well beyond their van der Waals surfaces that often correspond to crystallographic (*e.g.* NUHGED, Fig 9D) and other approximate translation symmetry operations. For this reason, such interactions (long M1) were disregarded when considering the supramolecular significance of each motif.

The remaining motifs, M2 – M4, were extracted from the 490 entries using the parameters ϕ > 40° and CC < 5.1Å. As shown in Fig. 9D, though less distinct than the subset depicting M1 motifs (Fig. 9C), the 77 hits retrieved provided well-defined signatures related to these assemblies. Structures that exhibit M2 and M4 patterns emerge as clusters at ϕ ~ 180° (Fig. 9D, red shaded entries). For M2 motifs, these clusters appear in the region of D2-D3 = 5.5Å and D1 = 7Å (28 hits, 19 refcodes), while M4 motifs cluster at D2-D3 = -1.5Å and D1 = 7Å (29 hits, 22 refcodes). Though other entries appear in these plot regions, without exception, those hits with ϕ ~ 180° (orange-red shading) represent pairs of TB molecules assembled into viable M2 or M4 motifs.

The crystal structure of (*rac*)-**2**-I provided our first exposure to motif M3. Though the fit of *endo*-face to *exo*-face arrangements that describe M3 patterns appears to be a logical extension of the M2 and M4 motifs, at the outset of this study it was unclear if this motif would emerge from our survey of other related structures. Close examination of Fig. 9D in the region of D2-D3 = 2 to 4 revealed 20 entries (12 refcodes) with similar ϕ values (50-80°). A thorough study of each entry in this subset revealed each molecular pair participating in M3 interactions. The 10 entry cluster near D1 = 4Å revealed intimate M3 contacts organized by effective π-stacking of adjacent aryl groups. Those entries with D1 > 5.5Å also form M3 motifs, however, the alignment of aryl groups in the majority of cases is slipped due to the steric affects from pendant functional groups.

By evaluating the various aspects of this structural study in its entirety, several general themes begin to emerge regarding the recognition profiles of TB compounds. Of the 112 structures included with this investigation, 58% (65 refcodes) organize using one or more of the motifs described in Scheme 2. A relatively even distribution of these molecular associations [short M1 (33 hits, 27 refcodes, M2 (29, 19), M3 (20, 12), and M4 (29, 22)] implies one motif does not offer considerable advantage over the others. Several structures prepared for this study align molecules using multiple motifs [(*R,R*)-**1**/(*S,S*)-**2**, [(*S,S*)-**2**/(*R,R*)-**3** and [(*S,S*)-**1**/(*rac*)-**3**]. The

notion of managing TB crystal structure using more than one packing synthon was observed in 14 of the database entries. This suggests a mixture of motifs is not only possible, but may lead to more effective packing under proper conditions. One example that combines motifs is the structure of quasiracemate (*R,R*)-**1**/(*S,S*)-**2** (Fig. 1), where the quasienantiomeric components assemble with a blend of M2 and M4 packing. This motif combination dominates the subset with 12 of the 14 entries and offers strong evidence for the complementary topologies of the M2/M4 supramolecular synthons. The remaining two entries crystallize by use of the M1/M4 (WAZTEY[41]) and M3/M4 (AZUTUL[42]) combinations.

We also explored the potential role of crystal symmetry to the frequency of motif formation. Considering both space group and motif symmetry it should follow that structures with inversion centers promote M2 and M4 molecular assemblies, while those organized with noncentrosymmetric packing prefer M1 and M3 alignment. For those structures containing short M1, M2, M3, or M4 motifs (80 structures), 41 exist in noncentrosymmetric space groups. And, further inspection reveals 56% (23 refcodes) contain on or more of the prescribed motifs. Nearly half of these structures assemble molecules in close proximity *via* translationally related M1 motifs (11 refcodes), with the remaining structures evenly dispersed over M2 (5), M3 (6), or M4 (5). A review of entries with centrosymmetric space groups (53 refcodes) showed a stronger penchant toward M2 and M4 motifs [M1 (16 refcodes), M2 (14), M3 (6), and M4 (17)] indicating a persuasive correlation between motif and crystallographic symmetry.

Conclusion

In summary, a family of 7 Tröger's base compounds that vary in configuration (quasiracemates, racemates, and enantiomers) and chemical substitutions (Me, Cl, and Br) has been investigated. The deliberate use of isosteric components provided a logical entry point to explore the quasiracemic behavior of TB compounds. The crystal structures of these quasiracemates contain several sets of molecular dimers organized by the complementary topologies of the quasienantiomeric components. These motifs closely mimic the centrosymmetric local environment observed with several racemic and solid-solution phases included with this study. Comparing this set of crystal structures to 105 entries found in the CSD revealed four distinct packing patterns - *i.e.,* M1 – M4 - retrieved using both TB···TB distance and orientation search criteria. Each motif takes advantage of the complementary topologies of the V-shaped building block and further highlights the importance of molecular shape to the recognition profile of these supramolecular assemblies. This approach exposed 58% of the entries (65 structures) exhibiting one or more of the pairwise relationships (short M1, M2, M3 or M4). Furthermore, those entries with noncentrosymmetric space groups tend to align pairs of molecules *via* asymmetric M1 motifs, while those crystallizing in centrosymmetric space groups follow M1 as well as the M2 and M4 symmetric motifs.

Acknowledgements

This work was supported by the National Science Foundation (CHE-0957391 and CHE-0722547) and a Council on Faculty Research Grant from Eastern Illinois University (EIU). We thank Prof. B. M. Foxman for key X-ray experimental contributions (NSF CHE-0521047). K.A.W. is grateful to the Cambridge Crystallographic Data Centre, Dr. S. Henderson (host), and EIU for generous sabbatical support.

Notes and references

‡ This paper was written in memoriam to the late Professor Raymond E. Davis (1938 to 2013), whose passion for crystallography and contributions to the field of quasiracemates is celebrated.

[a] Department of Chemistry, Eastern Illinois University, Charleston, Illinois, 61920, USA. E-mail: kawheeler@eiu.edu; Tel: +1 217 581 3119.

† Electronic supplementary information (ESI) available: Synthetic procedures and full crystal structure details and tables for (*R,R*)-**1**/(*S,S*)-**2**, (*S,S*)-**2**/(*R,R*)-**3**, (*S,S*)-**1**/(*S,S*)-**2**, (*S,S*)-**1**/(*rac*)-**3**, (*rac*)-**2**-I, (*rac*)-**2**-II, (*S,S*)-**4**·Cl, and **8**-Cl. Crystallographic database entries and tabulated motif search data. For ESI and crystallographic data in CIF or other electronic format see DOI: 10.1039/b000000x/

1 (*a*) *Acta Crystallogr., Sect. A,* 2013, **A69**, 1-69. [Bragg centennial themed issue]; (*b*) A. Authier, *Early Days of X-ray Crystallography*, Oxford University Press, USA, 2013; (*c*) D. W. Jones, *Contemp. Phys.*, 2013, **54**, 287-290; (*d*) G. R. Desiraju, *Angew. Chem., Int. Ed.*, 2014, **53**, 604-605; (*e*) W. Neumann, K.-W. Benz and H. Meskine, *Cryst. Res. Technol*., 2014, **49**, 1. (*f*) *Recent Advances in Crystallography*, Ed. J. Benedict, InTech, Croatia, 2012; (*g*) J. R. Helliwell, *Crystallogr. Rev.*, 2013, **18**, 108-116; (*h*) J. R. Helliwell, A. J. Blake, J. Blunden-Ellis, M. Moore, C. H. Schwalbe, *Crystallogr. Rev.*, 2012, **18**, 3-19.

2 W. H. Bragg and W. L. Bragg, *Proc. R. Soc. London, Ser. A*, 1913, **88**, 428-438.

3 J. D. Watson and F. H. C. Crick, *Nature*, 1953, **171**, 737-738.

4 M. F. Perutz, M. G. Rossmann, A. F. Cullis, H. Muirhead, G. Will, and A. C. T. North, *Nature*, 1960, **185**, 616-422.

5 D. C. Hodgkin, *Advancement Sci*., 1949, **6**, 85-89.

6 D. C. Hodgkin, J. P Pickworth, J. H. Robertson, K. N. Trueblood, R. J. P. Prosen and J. G. White, *Nature,* 1955, **176**, 325-328.

7 L. Pauling, *The Nature of the Chemical Bond*, Cornell University Press, USA, 1960.

8 K. Lonsdale, *Proc. R. Soc. London, Ser. A*, 1929, **123**, 494-515.

9 J. M. Bivoet, A. F. Peerdeman and A. J. van Bommel, *Nature*, 1951, **168**, 271-272.

10 H. B. Bürgi and J. D. Dunitz, *J. Am. Chem. Soc.*, 1973, **95**, 5065-5067.

11 J. Tröger, *J. Prakt. Chem*., 1887, **36**, 225-245.

12 (*a*) O. V. Runarsson, J. Artacho and K. Wärnmark, *Eur. J. Org. Chem.,* 2012, 7015-7041; (*b*) S. Sergeyev, *Helv. Chem. Acta*, 2009, **92**, 415-444; (*c*) B. Dolensky, M. Havlik and V. Kral, *Chem. Soc. Rev*., 2012, **41**, 3839-3858; (*d*) G. Kaupp, Tröger's Base Derivatives, in *Encyclopedia of Supramolecular Chemistry*, ed. J. L. Atwood and J. W. Steed. CRC Press, USA, Volume 2, 2004, 1516-1524.

13 M. A. Spielman, *J. Am. Chem. Soc*., 1935, **57**, 583-585.

14 S. B. Larson and C. S. Wilcox, *Acta Crystallogr., Sect. C: Cryst. Struct. Commun.*, 1986, **C42**, 224-227.

15 A search of the Cambridge Structural Database (Version 5.35, November 2013) tabulated the angle described by the aryl groups for structures containing the core Tröger's base framework, 6H,12H-5,11-methanodibenzo[b,f][1,5]diazocine. The search excluded oligo systems, compounds containing substituents attached to the central methylene group, and 6,12-dione adducts and resulted in 104 structures (131 hits) with clefts angles ranging from 90 – 113° (mean, 99.2(5.2)°).

16 (*a*) B. Dolenský, M. Havlík and V. Král, *Chem. Soc. Rev*., 2012, **41**, 3839-3858; (*b*) E. B. Veale and T. Gunnlaugsson, *J. Org. Chem*., 2010, **75**, 5513-5525; (*c*) S. Goswami, K. Ghosh and S. Dasgupta, *J. Org. Chem*., 2000, **65**, 1907-1914; (*d*) S. Goswami and K. Ghosh, *Tet. Lett*., 1997, **38**, 4503-4506; (*e*) E. M. Boyle, S. Comby, J. K. Molloy and T. Gunnlaugsson, *J. Org. Chem.*, 2013, **78**, 8312-8319; (*f*) A. Del Regno, A. Gonciaruk, L. Leay, M. Carta, M. Croad, R. Malpass-Evans, N. B. McKeown and F. R. Siperstein, *Ind. Eng. Chem. Res*., 2013, **52**, 16939-16950; (*g*) T. Kobayashi and T. Moriwaki, *Heterocycles,* 2004, **62**, 399-405; (*h*) E. B. Veale, D. O. Frimannsson, M. Lawler and T. Gunnlaugsson, *Org. Lett*., 2009, **11**, 4040-4043.

17 S. H. Wilen, J. Z. Qi and P. G. Williard, *J. Org. Chem*., 1991, **56**, 485-487.

18 (*a*) Y.-M. Shen, M.-X. Zhao, J. Xu and Y. Shi, *Angew. Chem., Int. Ed*., 2006, **45**, 8005-8008; (*b*) B. Minder, M. Schürch, T. Mallat and A. Baiker, *Catal. Lett*., 1995, **31**, 143-151; (*c*) F. Xu, R. D. Tilleyer, D. M. Tschaen, E. J. J. Grabowski and P. J. Reider, *Tetrahedron: Asymmetry*, 1998, **37**, 1651-1654; (*d*) M. Harmata and M. Kahraman, *Tetrahedron: Asymmetry*, 2000, **11**, 2875-2879; (*e*) Y. Goldberg and H. Alper, *Tet. Lett*., 1995, **36**, 369-372; (*f*) D. A. Lenev, K. A. Lyssenko and R. G. Kostyanovsky, *Russ. Chem. Bull.*, 2000, **49**, 1241-1244; (*g*) W. A. Herrmann, F. E. Kuhn, M. R. Mattner, G. R. J. Artus, M. R. Geisberger and J. D. G. Correia, *J. Organomet. Chem*., 1997, **538**, 203-209; (*h*) H. Wu, X.-M. Chen, Y. Wan, L. Ye, H.-Q. Xin, H.-H. Xu, C.-H. Yue, L.-L. Pang, R. Ma and D.-Q. Shi, *Tet. Lett*., 2009, **50**, 1062-1065.

19 (*a*) X. Du, Y. Sun, B. Tan, Q. Teng, X. Yao, C. Su and W. Wang, *Chem. Commun*., 2010, **46**, 970-972; (*b*) M. J. Crossley, T. W. Hambley, L. G. MacKay, A. C. Try and R. Walton, *Chem. Commun*., 1995, 1077-1079; (*c*) E. Poli, E. Merino, U. Díaz, D. Brunel and A. Corma, *J. Phys. Chem. C*, 2011, **115**, 7573-7585.

20 (*a*) Y. Lu, A. J. Bolokowicz, S. A. Reeb, J. D. Wiseman and K. A. Wheeler, *RSC Advances*, 2014, **4**, 8125-8131; (*b*) R. C. Grove, S. H. Malehorn, M. E. Breen and K. A. Wheeler, *Chem. Commun*., 2010, **46**, 7322-7324; (*c*) A. M. Lineberry, E. T. Benjamin, R. E. Davis, W. S. Kassel and K. A. Wheeler, *Cryst. Growth Des*., 2008, **8**, 612-619; (*d*) K. A. Wheeler, R. C. Grove, R. E. Davis and W. S. Kassel, *Angew. Chem., Int. Ed*., 2008, **47**, 78-81.

21 S. P. Kelley, L. Fábián and C. P. Brock, *Acta Crystallogr., Sect. B: Struct. Sci.*, 2011, **B67**, 79-93

22 H. Kooijman, A. L. Spek, A. Sobolev, H. Jongejan and M. C. R. Franssen, *Acta Crystallogr., Sect. E: Struct. Rep. Online*, 2002, **E58**, o532.

23 A. I. Kitaigorodskii, *Acta Crystallogr.*, 1965, **18**, 585-590.

24 (*a*) G. Lautrette, B. Kauffmann, Y. Ferrand, C. Aube, N. Chandramouli, D. Dubreuil and I. Huc, *Angew. Chem., Int. Ed*., 2013, **52**, 11517-11520; (*b*) C. Ebner, C. A. Muller, C. Markert and A. Pfaltz, Andreas, *J. Am. Chem. Soc*., 2011, **133**, 4710-4713; (*c*) F. Yang, J. J. Newsome and D. P. Curran, *J. Am. Chem. Soc*., 2006, **128**, 14200-14205.

25 (*a*) M. T. Reetz, *Angew. Chem. Int. Ed*., 2001, **40**, 284-310; (*b*) J. W. Faller, X. Liu, J. Parr, *Chirality*, 2000, **12**, 325-337; (*c*) S. Piovesana, Susy, R. Samperi, A. Lagana and M. Bella, *Chem. – Eur. J*., 2013, **19**, 11478-11494.

26 (*a*) E. Palovics, J. Schindler, F. Faigl and E. Fogassy, *Comprehensive Chirality*, ed. E. M. Carreira and H. Yamamoto, Elsevier, Amsterdam, 2012, **8**, 91-95; (*b*) N. A. Shaye, S. Chavda, E. Coulbeck, J. Eames and Y. Yohannes, *Tetrahedron: Asymmetry*, 2011, **22**, 439-463; (*c*) F. Cardona, D. Lalli, C. Faggi, A. Goti and A. Brandi, *J. Org. Chem*., 2008, **73**, 1999-2002.

27 (*a*) S. Akine, S. Hotate, T. Matsumoto and T. Nabeshima, *Chem. Commun.*, 2011, **47**, 2925-2927; (*b*) Q. Zhang, A. Rivkin and D. P. Curran, *J. Am. Chem. Soc*., 2002, **124**, 5774-5781.

28 (*a*) T. Jacobs, M. W. Bredenkamp, P. H. Neethling, E. G. Rohwer and L. J. Barbour, *Chem. Commun*., 2010, **46**, 8341-8343; (*b*) J. G. Nery, G. Bolbach, I. Weissbuch and M. Lahav, *Chem. – Eur. J*., 2005, **11**, 3039-3048.

29 C. F. Macrae, I. J. Bruno, J. A. Chisholm, P. R. Edgington, P. McCabe, E. Pidcock, L. Rodriguez-Monge, R. Taylor, J. van de Streek and P. A. Wood, *J. Appl. Cryst*., 2008, **41**, 466-470.

30 J. D. Field, P. Turner, M. M. Harding, T. Hatzikominosa and L. Kima, *New J. Chem*., 2002, **26**, 720-725.

31 (*a*) C. A. Hunter and J. K. M. Saunders, *J. Am. Chem. Soc*., 1990, **112**, 5525-5534; (*b*) M. Nishio, Y. Umezawa, K. Honda, S. Tsuboyama and H. Suezawa, *CrystEngComm,* 2009, **11**, 1757-1788; (*c*) C. E. Marjo, A. N. M. M. Rahman, R. Bishop, M. L. Scudder and D.C. Craig, *Tetrahedron*, 2001, **57**, 6289-6293; (*d*) A. N. M. M. Rahman, R. Bishop, D. C. Craig, C. E. Marjo and M. L. Scudder, *Cryst. Growth Des*., 2002, **2,** 421-426.

32 M. Faroughi, A. C. Try and P. Turner, *Acta Crystallogr., Sect. E: Struct. Rep. Online*, 2006, **E62**, o3674.

33 M. Faroughi, K.-X. Zhu, P. Jensen, D. C. Craig and A. C. Try, *Eur. J. Org. Chem.*, 2009, 4266-4272.

34 N. Ramasubbu, R. Parthasarathy and P. J. Murray-Rust, *J. Am. Chem. Soc.*, 1986, **108**, 4308-4314.

35 M. Faroughi, A. C. Try and P. Turner, *Acta Crystallogr., Sect. E: Struct. Rep. Online*, 2007, **E63**, o2695.

36 (*a*) E. C. Wagner, *J. Am. Chem. Soc*., 1935, **57**, 1296–1298; (*b*) E. C. Wagner, *J. Org. Chem*., 1954, **19**, 1862-1881; (*c*) C. A. M. Abella, M. Benassi, L. S. Santos, M. N. Eberlin and F. Coelho, *J. Org. Chem*., 2007, **72**, 4048-4054.

37 W.-W. Tian, S.-L. Dong, J.-Y. Xu, S. Ding and J.-T. Wang, *Acta Crystallogr., Sect. E: Struct. Rep. Online*, 2007, **E63**, o4734.

38 M. D. H. Bhuiyan, J. K. Clegg and A. C. Try, *Acta Crystallogr., Sect. E: Struct. Rep. Online*, 2007, **E63**, o308.

39 C. A. M. Abella, M. Benassi, L. S. Santos, M. N. Eberlin and F. Coelho, *J. Org. Chem*., 2007, **72**, 4048-4054.

40 I. J. Bruno, J. C. Cole, P. R. Edgington, M. Kessler, C. F. Macrae, P. McCabe, J. Pearson and R. Taylor, *Acta Crystallogr., Sect. B: Struct. Sci.*, 2002, **B58**, 389-397.

41 C. Benkhauser-Schunk, B. Wezisla, K. Urbahn, U. Kiehne, J. Daniels, G. Schnakenburg, F. Neese and A. Lutzen, *ChemPlusChem*, 2012, **77**, 396-403.

42 Y. Xu, S. Jin, J, Zhu, Y, Liu and C, Shi, *Acta Crystallogr., Sect. E: Struct. Rep. Online*, 2011, **E67**, o2730.

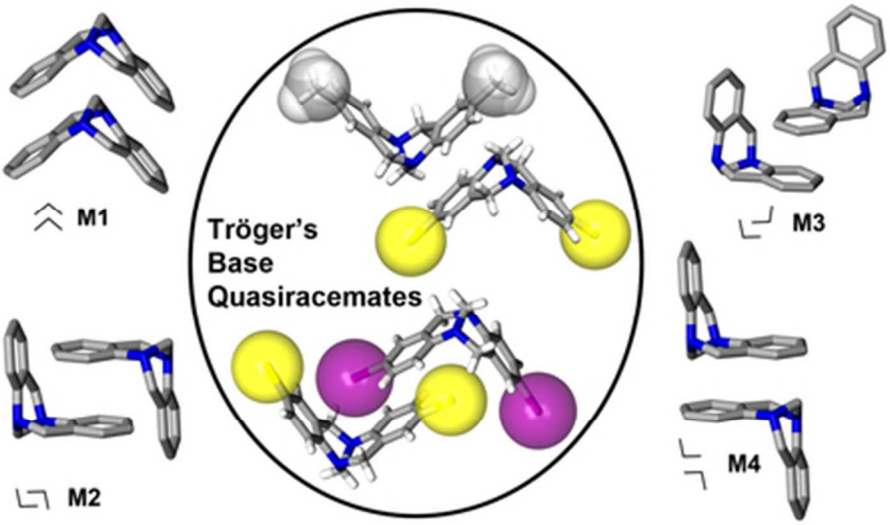

Comparison of a family of Tröger's base compounds to the CSD reveals four distinct dimeric packing motifs due to the complementary topologies of the components.
39x22mm (300 x 300 DPI)